Computationally Efficient Multi-Fidelity Multi-Grid Design Optimization of Microwave Structures

Slawomir Koziel

Engineering Optimization & Modeling Center, School of Science and Engineering,
Reykjavik University, 101 Reykjavik, Iceland
koziel@ru.is

***Abstract*—** A simple and reliable algorithm for design optimization of microwave structures is introduced. The presented methodology exploits coarse-discretization models of the structure of interest, starting from a very coarse mesh, and gradually increases the discretization density. Each model is optimized using a simple grid-search routine. The optimal design of the current model is used as an initial design for the finer-discretization one. The proposed methodology is computationally efficient as most of the operations are performed on coarse-discretization models. Three examples of microstrip filter designs are given.

***Index Terms*—** Computer-aided design (CAD), electromagnetic simulation, derivative-free optimization, grid search, microwave design.

I. INTRODUCTION

Due to the complexity of microwave structures and a growing demand for accuracy, theoretical models can only be used to yield initial designs that need to be further tuned to meet given performance specifications. Therefore, EM-simulation-based design closure becomes increasingly important. A serious bottleneck of simulation-driven optimization is its high computational cost, which makes straightforward approaches such as employing EM solvers directly in an optimization loop impractical. Co-simulation [1-3] is only a partial solution because the circuit models with embedded EM components are still directly optimized.

Efficient simulation-driven design can be realized using a surrogate-based optimization (SBO) principle [4], [5], where the optimization burden is shifted to a surrogate model, computationally cheap representation of the structure being optimized (referred to as the fine model). The successful SBO approaches used in microwave area include space mapping (SM) [6-12] and various forms of tuning [13-15] and tuning SM [16], [17]. Unfortunately, their implementation is not always straightforward: substantial modification of the optimized structure may be required (tuning), or additional mapping and more or less complicated interaction between auxiliary models is necessary (SM). Also, space mapping performance heavily depends on the proper selection of the surrogate model and its parameters [18].

Here, a simple yet efficient design optimization methodology is introduced. Our technique is based on iterative optimization of coarse-discretization models using a simple grid-search algorithm. The optimal design of the current model is used as an initial design for the finer-discretization one. The final design can be refined using a second-order polynomial approximation of the available EM-simulation data.

The proposed methodology is very simple to implement. Unlike space mapping or other surrogate-based approaches, it does not require a circuit-equivalent coarse model or any modification of the structure being optimized. It is also computationally efficient because the optimization burden is shifted to the coarsely-discretized models. As our technique is based on a grid-search routine, it allows design optimization of structures simulated with solvers using structured grids such as Sonnet ***em*** [19].

II. MULTI-FIDELITY MULTI-GRID DESIGN OPTIMIZATION

In this section, we formulate the optimization problem (Section II.A), describe the building blocks of the proposed optimization procedure (Sections II.B-II.E), formulate the procedure (Section II.F), and discuss some practical issues (Section II.G).

A. Design Optimization Problem

The design optimization problem is formulated as follows:

$$\boldsymbol{x}_f^* = \arg\min_{\boldsymbol{x}} U\left(\boldsymbol{R}_f(\boldsymbol{x})\right) \quad (1)$$

where $\boldsymbol{R}_f \in R^m$ denotes the response vector of a fine model of the device of interest, e.g., the modulus of the reflection coefficient $|S_{21}|$ evaluated at m different frequencies; $\boldsymbol{x} \in R^n$ is a vector of design variables, and U is a given scalar merit function, e.g., a minimax function with upper and lower specifications. Vector $\boldsymbol{x}_f^*$ is the optimal design to be determined.

As mentioned in the introduction, the fine model is assumed to be computationally expensive so that its straightforward optimization (e.g., using gradient-based search) is prohibitive because of high computational cost.

Here, the fine model is evaluated on a simulation grid $d_{1.f} \times d_{2.f} \times \ldots \times d_{n.f}$ that determines the resolution of the design optimization process (see Fig. 3 for illustration). In case of Sonnet ***em***, $d_{k.f}$ is equal to either $g_{h.f}$ or $g_{v.f}$ (the horizontal or vertical cell size used by the EM solver).

$\boldsymbol{x}^{(j)} = s(\boldsymbol{x}^{(j-1)})$; // Snap $\boldsymbol{x}^{(j)}$ to the nearest grid point
$U_{min} = U(\boldsymbol{R}_{c.f}(\boldsymbol{x}^{(j)}))$; // Evaluate objective function
do
  $U_0 = U_{min}$; // Update the reference objective function value
  for $k = 1$ to n // Evaluating objective function at perturbed designs
    $U_k = U(\boldsymbol{R}_{c.f}([x_1^{(j)} \ldots x_k^{(j)} + d_{k.j} \ldots x_n^{(j)}]^T))$; // (here, $d_k = g_{h.j}$ or $g_{v.j}$ (depends on orientation of $x_k^{(j)}$))
  end
  $\boldsymbol{h} = -[(U_1 - U_0)/d_{1.j} \ldots [(U_n - U_0)/d_{n.j}]^T$; // Search direction estimation
  $\boldsymbol{h} = \boldsymbol{h} \cdot (\|[d_{1.j} \ldots d_{n.j}]^T\|/\|\boldsymbol{h}\|)$; // Search direction normalization
  do // Line search:
    $\boldsymbol{x}_{tmp} = s(\boldsymbol{x}^{(j)} + \boldsymbol{h})$; // Set the trial design and "snap" it to the grid
    $U_{tmp} = U(\boldsymbol{R}_{c.f}(\boldsymbol{x}_{tmp}))$; // Evaluate objective function at the trial design
    if $U_{tmp} < U_{min}$ // If the trial is successful:
      $\boldsymbol{x}^{(j)} = \boldsymbol{x}_{tmp}$; // 1. Update the design
      $U_{min} = U_{tmp}$; // 2. Store the best result
      $\boldsymbol{h} = 2 \cdot \boldsymbol{h}$; // 3. Increase the search step
    else
      break; // Otherwise, exit the line search algorithm
    end
  while 1
  if $U_{min} \geq U_0$ // Line search failed => perform local search
    for $k = 1$ to n
      $U_{-k} = U(\boldsymbol{R}_{c.f}([x_1^{(j)} \ldots x_k^{(j)} - d_{k.j} \ldots x_n^{(j)}]^T))$; // Evaluate the remaining neighbours of $\boldsymbol{x}^{(j)}$
    end
    $U_{tmp} = \min\{U_{-k}, U_{-k+1}, \ldots, U_{k-1}, U_k\}$; // Find the best design
    $k_{tmp} = \text{argmin}\{-n \leq k \leq n : U_k\}$; // Fine the corresponding perturbation index
    if $U_{min} < U_0$ // If local search is successful:
      $\boldsymbol{x}^{(j)} = [x_1^{(j)} \ldots x_k^{(j)} + \text{sign}(k_{tmp}) \cdot d_{k.j} \ldots x_n^{(j)}]^T$; // 1. Update the design
      $U_{min} = U_{k_{tmp}}$; // 2. Store the best value
    end
  end
while $U_{min} < U_0$ // Continue if further improvement was possible
return $\boldsymbol{x}^{(j)}$; // Otherwise, return $\boldsymbol{x}^{(j)}$ as the optimal design of $\boldsymbol{R}_{c.j}$

Fig. 1. Pseudo-code of the grid-search algorithm.

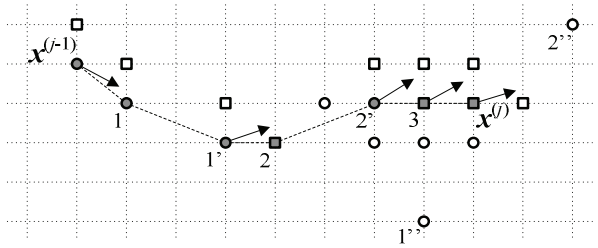

Fig. 2. Illustration of the grid-search algorithm for two design variables (n = 2). The search direction ($\rightarrow$) at the initial design $\boldsymbol{x}^{(j-1)}$ is obtained using two perturbed designs marked as squares. The trial points for the line search are denoted as 1, 1' and 1''. The last successful trial design is 1'. At this design, a new search direction is found, and a new line search is launched with designs 2, 2' and 2'' (the last of which is unsuccessful). The next line search starting from 2' is unsuccessful and the new design 3 is obtained using a local search, similarly as the final design $\boldsymbol{x}^{(j)}$ that cannot be further improved even by a local search, which terminates the algorithm.

B. Coarse-Discretization Models

The optimization technique introduced here exploits a family of coarse-discretization models $\{\boldsymbol{R}_{c.j}\}$, $j = 1, \ldots, K$, all evaluated using the same EM solver. The model $\boldsymbol{R}_{c.j}$ exploits a simulation grid $d_{1.j} \times d_{2.j} \times \ldots \times d_{n.j}$. It is assumed that $d_{k.j} > d_{k.j+1}$ and for $k = 1, \ldots, n$ and $j = 1, \ldots, K-1$, and $d_{k.K} > d_{k.f}$ for all k. In other words, discretization of $\boldsymbol{R}_{c.j+1}$ is finer than that of $\boldsymbol{R}_{c.j}$. It is recommended that $d_{k.j}/d_{k.j+1}$ is an integer (typically 2 or 3). In practice, the number K of coarse-discretization models is two or three.

C. Grid-Search Algorithm

To optimize the coarse-discretization model $\boldsymbol{R}_{c.j}$ we use the grid-search procedure shown in Fig. 1. Here, $\boldsymbol{x}^{(j-1)} = [x_1^{(j-1)} \ \ldots \ x_n^{(j-1)}]^T$ is the initial design, i.e., the optimal design of $\boldsymbol{R}_{c.j-1}$, s is a function that "rounds" $\boldsymbol{x}$ to the nearest grid point $s(\boldsymbol{x})$).

For simplicity, only the unconstrained version of the grid-search algorithm is described here. The generalization for constrained optimization is straightforward. The operation of the algorithm is illustrated in Fig. 2.

D. Design Refinement

Having optimized the finest of the coarse-discretization models, $\boldsymbol{R}_{c.K}$, we also have its evaluations at $\boldsymbol{x}^{(K)}$ and at all perturbed designs around it $\boldsymbol{x}_k^{(K)} = [x_1^{(K)} \ \ldots \ x_k^{(K)} + \text{sign}(k)\cdot d_{k.K} \ \ldots \ x_n^{(K)}]^T$, i.e., $\boldsymbol{R}^{(k)} = \boldsymbol{R}_{c.K}(\boldsymbol{x}_k^{(K)})$, $k = -n, -n+1, \ldots, n-1, n$. This data can be used to refine the final design without directly optimizing $\boldsymbol{R}_f$. Instead, one can set up an approximation model involving $\boldsymbol{R}^{(k)}$ and optimize it in the neighbourhood of $\boldsymbol{x}^{(K)}$ defined as $[\boldsymbol{x}^{(K)} - \boldsymbol{d}, \boldsymbol{x}^{(K)} + \boldsymbol{d}]$, where $\boldsymbol{d} = [d_{1.K} \ d_{2.K} \ \ldots \ d_{n.K}]^T$. In this work, we use a reduced quadratic model $\boldsymbol{q}(\boldsymbol{x}) = [q_1 \ q_2 \ \ldots \ q_m]^T$, defined as

$$q_j(\boldsymbol{x}) = q_j([x_1 \ldots x_n]^T) = \lambda_{j.0} + \lambda_{j.1}x_1 + \ldots + \ldots + \lambda_{j.n}x_n + \lambda_{j.n+1}x_1^2 + \ldots + \lambda_{j.2n}x_n^2 \quad (2)$$

Coefficients $\lambda_{j.r}$, $j = 1, \ldots, m$, $r = 0, 1, \ldots, 2n$, can be uniquely obtained by solving the linear regression problems $q_j(\boldsymbol{x}_k^{(K)}) = R_j^{(k)}$, $k = -n, -n+1, \ldots, n-1, n$, where $R_j^{(k)}$ is a jth component of the vector $\boldsymbol{R}^{(k)}$.

In order to account for possible misalignment between $\boldsymbol{R}_{c.K}$ and $\boldsymbol{R}_f$, it is recommended—instead of optimizing the quadratic model $\boldsymbol{q}$—to optimize a corrected model $\boldsymbol{q}(\boldsymbol{x}) + [\boldsymbol{R}_f(\boldsymbol{x}^{(K)}) - \boldsymbol{R}_{c.K}(\boldsymbol{x}^{(K)})]$ that ensures a zero-order consistency [20] between $\boldsymbol{R}_{c.K}$ and $\boldsymbol{R}_f$. The refined design can be then found as

$$\boldsymbol{x}^* = \arg\min\{\boldsymbol{x}^{(K)} - \boldsymbol{d} \le \boldsymbol{x} \le \boldsymbol{x}^{(K)} + \boldsymbol{d} : U(\boldsymbol{q}(\boldsymbol{x}) + [\boldsymbol{R}_f(\boldsymbol{x}^{(K)}) - \boldsymbol{R}_{c.K}(\boldsymbol{x}^{(K)})])\} \quad (3)$$

If necessary, the step (3) can be performed a few times starting from a refined design, i.e., $\boldsymbol{x}^* = \text{argmin}\{\boldsymbol{x}^{(K)} - \boldsymbol{d} \le \boldsymbol{x} \le \boldsymbol{x}^{(K)} + \boldsymbol{d} : U(\boldsymbol{q}(\boldsymbol{x}) + [\boldsymbol{R}_f(\boldsymbol{x}^*) - \boldsymbol{R}_{c.K}(\boldsymbol{x}^*)])\}$ (each iteration requires only one evaluation of $\boldsymbol{R}_f$).

E. Optional Design Specifications Adjustments

Typically, the major difference between the responses of $\boldsymbol{R}_f$ and coarse-discretization models $\boldsymbol{R}_{c.j}$ is that they are shifted in frequency. This difference can be easily absorbed by frequency-shifting the design specifications while optimizing a model $\boldsymbol{R}_{c.j}$. More specifically, suppose that the design specifications are described as $\{\omega_{k.L}, \omega_{k.H}; s_k\}$, $k = 1, \ldots, n_s$, (e.g., specifications $|S_{21}| \ge -3$ dB for 3 GHz $\le \omega \le 4$ GHz, $|S_{21}| \le -20$ dB for 1 GHz $\le \omega \le 2$ GHz and $|S_{21}| \le -20$ dB for 5 GHz $\le \omega \le 7$ GHz would be described as {3, 4; –3}, {1, 2; –20}, and {5, 7; –20}). If the average frequency shift between responses of $\boldsymbol{R}_{c.j}$ and $\boldsymbol{R}_{c.j+1}$ is $\Delta\omega$, this difference can be absorbed by modifying the design specifications to $\{\omega_{k.L} - \Delta\omega, \omega_{k.H} - \Delta\omega, s_k\}$, $k = 1, \ldots, n_s$.

F. Optimization Algorithm

The optimization procedure proposed in this work can be summarized as follows (input arguments are: initial design $\boldsymbol{x}^{(0)}$ and the number of coarse-discretization models K):

1. Set $j = 1$;
2. Optimize $\boldsymbol{R}_{c.j}$ using the algorithm of Section 2.*B* to obtain a new design $\boldsymbol{x}^{(j)}$;
3. Set $j = j + 1$; if $j < K$ go to 2;
4. Set up a quadratic model $\boldsymbol{q}$ as in (2) and find a refined design $\boldsymbol{x}^*$ using (3).

Note that the original model $\boldsymbol{R}_f$ is only evaluated at the final stage (step 4) of the optimization process. Operation of our optimization procedure is illustrated in Fig. 3.

G. Selection of the Coarse-Discretization Models

As mentioned in Section II.*B*, the number K of coarse-discretization models is typically two or three. The first coarse-discretization model $\boldsymbol{R}_{c.1}$ should be set up so that its evaluation time is at least 30 to 100 times shorter than the evaluation time of the fine model. The reason is that the initial design may be quite poor so that the expected number of evaluations of $\boldsymbol{R}_{c.1}$ is usually large. By keeping $\boldsymbol{R}_{c.1}$ fast, one can control the computational overhead related to its optimization. Accuracy of $\boldsymbol{R}_{c.1}$ is not critical because its optimal design is only supposed to give a rough estimate of the fine model optimum.

The second (and, possibly third) coarse-discretization model should be more accurate but still at least about 10 times faster than the fine model. This can be achieved by proper manipulation of the EM solver mesh density.

III. EXAMPLES

A. Compact Stacked Slotted Resonators Microstrip Bandpass Filter [21]

Consider the stacked slotted resonators bandpass filter [21] shown in Fig. 4. The design parameters are $\boldsymbol{x} = [L_1\ L_2\ W_1\ S_1\ S_2\ d]^T$ mm. The filter is simulated in Sonnet ***em*** [19] using a cell size of 0.05 mm × 0.05 mm (model $\boldsymbol{R}_f$), which corresponds to a simulation grid $d_{1.f} \times d_{2.f} \times \ldots \times d_{n.f}$ of 0.05 × 0.05 × … × 0.05 mm. The design specifications are $|S_{21}| \geq -3$ dB for 2.35 GHz ≤ ω ≤ 2.45 GHz, and $|S_{21}| \leq -20$ dB for 1.9 GHz ≤ ω ≤ 2.3GHz and 2.6 GHz ≤ ω ≤ 2.9 GHz. The initial design is $\boldsymbol{x}^{(0)} = [7\ 10\ 0.6\ 1\ 2\ 1]^T$ mm.

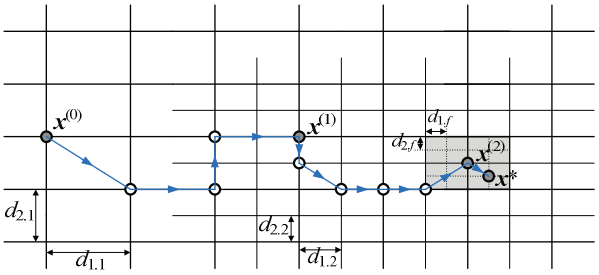

Fig. 3. Operation of the proposed optimization procedure for $n = 2$ and $K = 2$: Optimized design $\boldsymbol{x}^{(1)}$ of the model $\boldsymbol{R}_{c.1}$ is found on the grid $d_{1.1} \times d_{2.1}$ starting from the initial design $\boldsymbol{x}^{(0)}$. Then, the optimized design $\boldsymbol{x}^{(2)}$ of $\boldsymbol{R}_{c.2}$ is searched for on the grid $d_{2.2} \times d_{2.2}$ using $\boldsymbol{x}^{(1)}$ as the initial design. Finally, the design $\boldsymbol{x}^{(2)}$ is refined (cf. (3)) on the fine grid $d_{1.f} \times d_{2.f}$ using a second-order polynomial model (2) that is set up in the shaded area around $\boldsymbol{x}^{(2)}$.

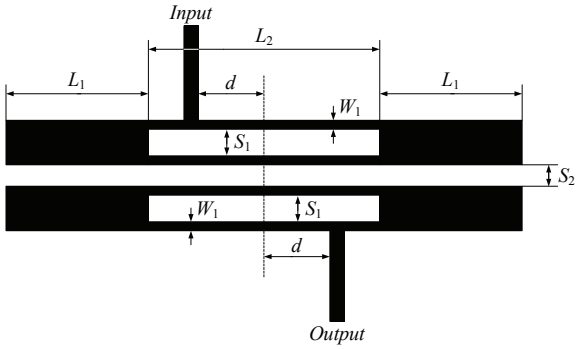

Fig. 4. Stacked slotted resonators filter: geometry [21].

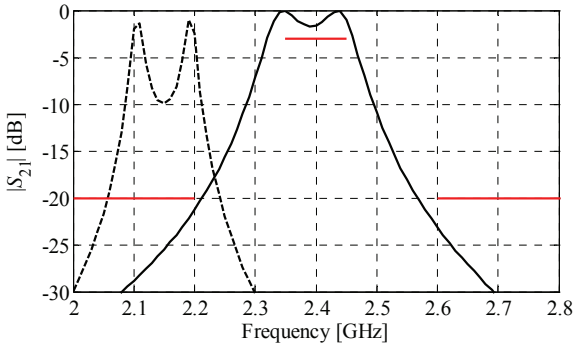

Fig. 5. Stacked slotted resonators filter: responses of the coarse-discretization model $\boldsymbol{R}_{c.1}$ (0.2 mm × 0.2 mm grid) at the initial design $\boldsymbol{x}^{(0)}$ (dashed line) and at the optimized design of $\boldsymbol{R}_{c.1}$, $\boldsymbol{x}^{(1)}$, (solid line).

Table 1: Optimization cost of the stacked slotted resonators bandpass filter.

Algorithm Component	Number of Model Evaluations	Evaluation Time	
		Absolute [min]	Relative to $\boldsymbol{R}_f$
Optimization of the coarse-discretization model $\boldsymbol{R}_{c.1}$	41	49	3.1
Optimization of the coarse-discretization model $\boldsymbol{R}_{c.2}$	26	130	8.1
Evaluation of the original (fine-discretization) model $\boldsymbol{R}_f$	2	32	2.0
Total optimization time	N/A	211	13.2

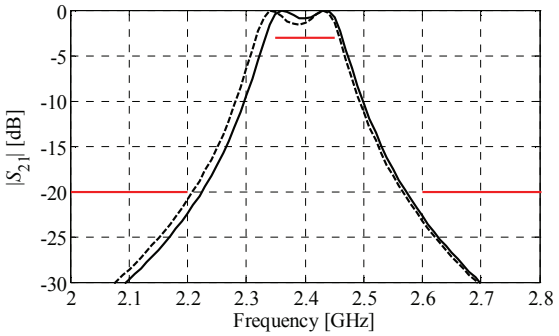

Fig. 6. Stacked slotted resonators filter: responses of the coarse-discretization model $\boldsymbol{R}_{c.2}$ (0.05 mm × 0.2 mm grid) at $\boldsymbol{x}^{(1)}$ (dashed line) and at $\boldsymbol{x}^{(2)}$ (solid line), the optimized design of $\boldsymbol{R}_{c.2}$ found using a grid search.

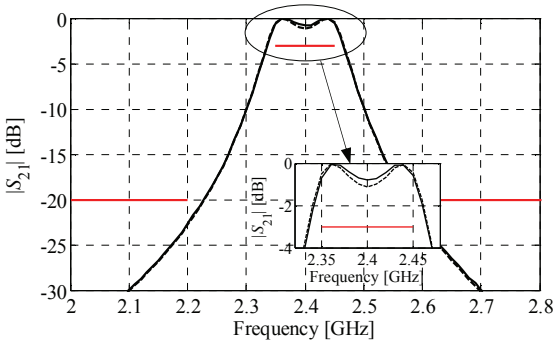

Fig. 7. Stacked slotted resonators filter: responses of the original fine-discretization model $\boldsymbol{R}_f$ at $\boldsymbol{x}^{(2)}$ (dashed line) and at the refined final design $\boldsymbol{x}^*$ (solid line).

The proposed multi-fidelity multi-grid design optimization procedure is realized here using two coarse-discretization models: $\boldsymbol{R}_{c.1}$ (cell size 0.2 mm × 0.2 mm, simulation grid $0.2 \times 0.2 \times \ldots \times 0.2$ mm) and $\boldsymbol{R}_{c.2}$ (cell size 0.05 mm × 0.2 mm, simulation grid 0.05 × 0.05 × 0.2 × 0.2 × 0.2 × 0.05 mm). The evaluation times for $\boldsymbol{R}_{c.1}$, $\boldsymbol{R}_{c.2}$ and $\boldsymbol{R}_f$ are 72 s, 5 min and 16 min, respectively.

Figure 5 shows the responses of $\boldsymbol{R}_{c.1}$ at $\boldsymbol{x}^{(0)}$ and at $\boldsymbol{x}^{(1)} = [6.4\ 9.6\ 0.6\ 0.6\ 2\ 1.8]^T$ mm, its optimal design found using a grid search. Figure 6 shows the responses of $\boldsymbol{R}_{c.2}$ at $\boldsymbol{x}^{(1)}$ and at its optimized design $\boldsymbol{x}^{(2)} = [6.35\ 9.6\ 0.6\ 0.6\ 2.2\ 1.8]^T$ mm. Figure 7 shows the responses of $\boldsymbol{R}_f$ at $\boldsymbol{x}^{(2)}$ (specification error –1.7 dB) and the refined design $\boldsymbol{x}^* = [6.35\ 9.6\ 0.6\ 0.6\ 2.25\ 1.85]^T$ mm (specification error –2.1 dB). The total optimization cost (Table 1) is quite low and corresponds to only 13 evaluations of the original, fine-discretization model. Most of this cost is due to the optimization of the coarse-discretization model $\boldsymbol{R}_{c.2}$.

B. High-Temperature Superconducting Filter [22]

As the second example, consider the high-temperature superconducting (HTS) filter shown in Fig. 8 [22]. The design parameters are $\boldsymbol{x} = [L_1\ L_2\ L_3\ S_1\ S_2\ S_3]^T$. The width of all the sections is $W = 8$ mil. A substrate of lanthanum aluminate is used with $\varepsilon_r = 23.425$ $H = 20$ mil. The filter is simulated in Sonnet ***em*** [19] using a grid of 0.5 mil × 0.5 mil (the $\boldsymbol{R}_f$ model). The design specifications are $|S_{21}| \leq 0.05$ for $\omega \leq 3.966$ GHz, $|S_{21}| \geq 0.95$ for 4.008 GHz $\leq \omega \leq 4.058$ GHz, and $|S_{21}| \leq 0.05$ for $\omega \geq 4.100$ GHz. The initial design is $\boldsymbol{x}^{(0)} = [196\ 196\ 190\ 20\ 92\ 100]^T$ mil.

Again, we use two coarsely discretized models: $\boldsymbol{R}_{c.1}$ (grid of 2 mil × 4 mil) and $\boldsymbol{R}_{c.2}$ (grid of 1 mil × 2 mil). The evaluation times for $\boldsymbol{R}_{c.1}$, $\boldsymbol{R}_{c.2}$ and $\boldsymbol{R}_f$ are about 2 min, 6 min and 51 min, respectively. Figure 9 shows the responses of $\boldsymbol{R}_{c.1}$ at $\boldsymbol{x}^{(0)}$ and at $\boldsymbol{x}^{(1)} = [188\ 190\ 188\ 20\ 76\ 84]^T$ mil, its optimal design found using a grid search, as well as the response of $\boldsymbol{R}_{c.2}$ at $\boldsymbol{x}^{(0)}$. Because of noticeable frequency shift between $\boldsymbol{R}_{c.1}(\boldsymbol{x}^{(0)})$ and $\boldsymbol{R}_{c.2}(\boldsymbol{x}^{(0)})$ (7 MHz on average) the design specifications were adjusted as described in Section II.*E* while optimizing $\boldsymbol{R}_{c.1}$. Figure 10 shows the responses of $\boldsymbol{R}_{c.2}$ at $\boldsymbol{x}^{(1)}$ and at its optimized design $\boldsymbol{x}^{(2)} = [188\ 189\ 188\ 20\ 76\ 86]^T$ mil, as well as the response of $\boldsymbol{R}_f$ at $\boldsymbol{x}^{(2)}$. Here, the average frequency shift between $\boldsymbol{R}_{c.2}(\boldsymbol{x}^{(1)})$ and $\boldsymbol{R}_f(\boldsymbol{x}^{(1)})$ is about 5 MHz

Table 2: Optimization cost of the HTS filter.

Algorithm Component	Number of Model Evaluations	Evaluation Time	
		Absolute [min]	Relative to $\boldsymbol{R}_f$
Optimization of the coarse-discretization model $\boldsymbol{R}_{c.1}$	104	195	3.8
Optimization of the coarse-discretization model $\boldsymbol{R}_{c.2}$	26	152	3.0
Evaluation of the original (fine-discretization) model $\boldsymbol{R}_f$	3	153	3.0
Total optimization time	N/A	500	9.8

Table 3: Optimization cost of the coupled-line bandpass filter.

Algorithm Component	Number of Model Evaluations	Evaluation Time	
		Absolute [min]	Relative to $\boldsymbol{R}_f$
Optimization of the coarse-discretization model $\boldsymbol{R}_{c.1}$	82	42	1.0
Optimization of the coarse-discretization model $\boldsymbol{R}_{c.2}$	55	276	6.4
Evaluation of the original (fine-discretization) model $\boldsymbol{R}_f$	2	86	2.0
Total optimization time	N/A	404	9.4

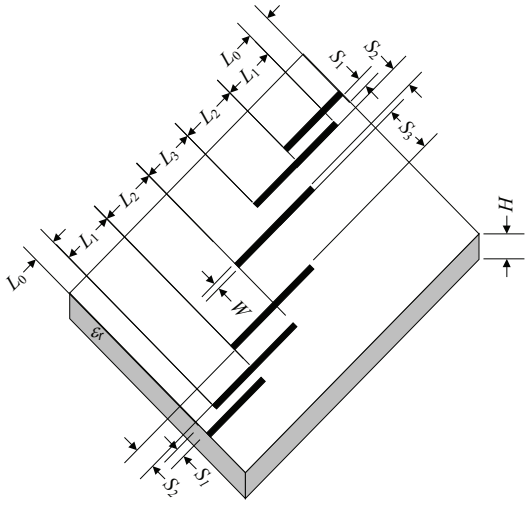

Fig. 8. HTS filter: geometry [22].

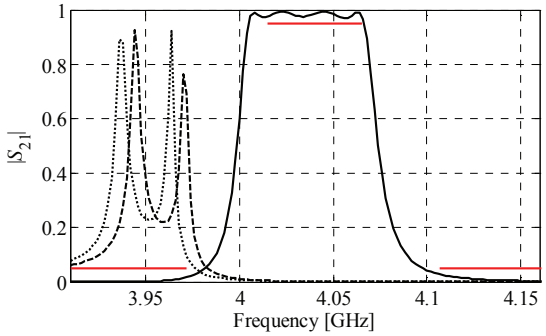

Fig. 9. HTS filter: responses of the coarse-discretization model $\boldsymbol{R}_{c.1}$ at the initial design $\boldsymbol{x}^{(0)}$ (dashed line) and at its optimized design $\boldsymbol{x}^{(1)}$ (solid line), as well as the response of $\boldsymbol{R}_{c.2}$ at $\boldsymbol{x}^{(0)}$ (dotted line); design specifications are shifted by 7 MHz towards higher frequencies to absorb the frequency shift between $\boldsymbol{R}_{c.1}(\boldsymbol{x}^{(0)})$ and $\boldsymbol{R}_{c.2}(\boldsymbol{x}^{(0)})$.

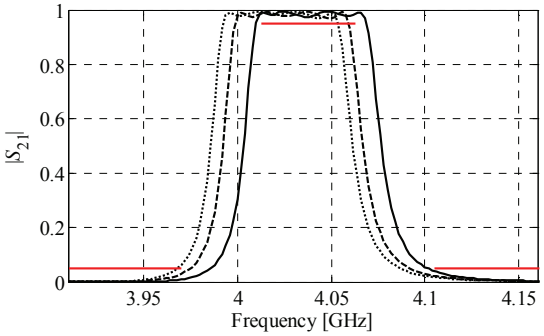

Fig. 10. HTS filter: responses of the coarse-discretization model $\boldsymbol{R}_{c.2}$ at $\boldsymbol{x}^{(1)}$ (dashed line) and at its optimized design $\boldsymbol{x}^{(2)}$ (solid line), as well as the response of $\boldsymbol{R}_f$ at $\boldsymbol{x}^{(2)}$ (dotted line); design specifications are shifted by 5 MHz toward higher frequencies to absorb the frequency shift between $\boldsymbol{R}_{c.2}(\boldsymbol{x}^{(1)})$ and $\boldsymbol{R}_f(\boldsymbol{x}^{(1)})$.

and the design specifications are modified accordingly. Figure 11 shows the responses of $\boldsymbol{R}_f$ at $\boldsymbol{x}^{(2)}$ (specification error –0.01) and the refined design $\boldsymbol{x}^* = [188\ 189\ 188\ 20.5\ 78\ 88]^T$ mm (specification error –0.02). Total optimization cost (Table 2) corresponds to only 10 evaluations of the fine-discretization model.

C. Coupled-Line Microstrip Bandpass Filter [23]

Consider the coupled-line bandpass filter [23] shown in Fig. 12. The design parameters are $\boldsymbol{x} = [L_1\ L_2\ L_3\ L_4\ S_1\ S_2]^T$ mm. The fine model $\boldsymbol{R}_f$ is simulated in FEKO [24]. The initial design is $\boldsymbol{x}^{(0)} = [18.0\ 7.0\ 15.0\ 10.0\ 0.2\ 0.2]^T$ mm. The total mesh number for $\boldsymbol{R}_f$ at the initial design is 1422.

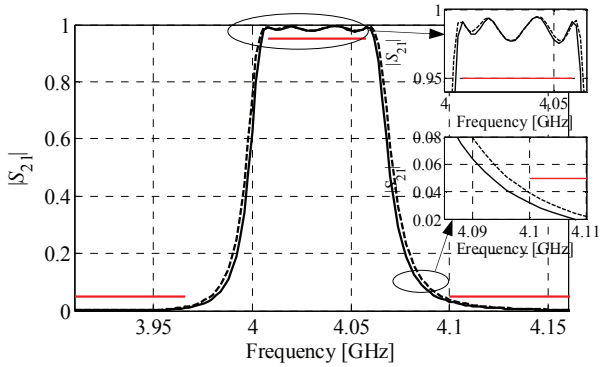

Fig. 11. HTS filter: responses of the fine-discretization model $\boldsymbol{R}_f$ at $\boldsymbol{x}^{(2)}$ (dashed line) and at the refined final design $\boldsymbol{x}^*$ (solid line); here the original design specifications are shown.

The design specifications are $|S_{21}| \geq -1$ dB for 2.35 GHz $\leq \omega \leq$ 2.45 GHz, and $|S_{21}| \leq -20$ dB for 1.5 GHz $\leq \omega \leq$ 2.25GHz and 2.55 GHz $\leq \omega \leq$ 3.3 GHz.

We are using two coarse models: $\boldsymbol{R}_{c.1}$ (total mesh number 160 at $\boldsymbol{x}^{(0)}$, simulation grid 0.1 × 0.1 × 0.1 × 0.1 × 0.02 × 0.02 mm) and $\boldsymbol{R}_{c.2}$ (total mesh number 678 at $\boldsymbol{x}^{(0)}$, simulation grid 0.05 × 0.05 × 0.05 × 0.05 × 0.01 × 0.01 mm). The evaluation times for $\boldsymbol{R}_{c.1}$, $\boldsymbol{R}_{c.2}$ and $\boldsymbol{R}_f$ are about 30 seconds, 5 min and 43 min, respectively. Figure 13 shows the responses of $\boldsymbol{R}_{c.1}$ at $\boldsymbol{x}^{(0)}$ and at $\boldsymbol{x}^{(1)} = [18.0\ 7.0\ 13.8\ 10.2\ 0.2\ 0.1]^T$ mm, as well as the response of $\boldsymbol{R}_{c.2}$ at $\boldsymbol{x}^{(0)}$. Because of the frequency shift between $\boldsymbol{R}_{c.1}(\boldsymbol{x}^{(0)})$ and $\boldsymbol{R}_{c.2}(\boldsymbol{x}^{(0)})$, the design specifications were adjusted accordingly (cf. Section II.*E*) while optimizing $\boldsymbol{R}_{c.1}$. Figure 14 shows the responses of $\boldsymbol{R}_{c.2}$ at $\boldsymbol{x}^{(1)}$ and at its optimized design $\boldsymbol{x}^{(2)} = [18.0\ 7.0\ 13.7\ 10.2\ 0.18\ 0.12]^T$ mm, as well as the response of $\boldsymbol{R}_f$ at $\boldsymbol{x}^{(2)}$. Figure 15 shows the responses of $\boldsymbol{R}_f$ at $\boldsymbol{x}^{(2)}$ (specification error +0.02 dB) and the refined design $\boldsymbol{x}^* = [17.994\ 7.013\ 13.663\ 10.138\ 0.128\ 0.118]^T$ mm (specification error –0.74 dB). Note that, in this case, the refinement step (3) was not constrained to the simulation grid.

Total optimization cost (Table 3) corresponds to less than 10 evaluations of the fine-discretization model. Similarly as for the first test problem, optimization of the second coarse-discretization model $\boldsymbol{R}_{c.2}$ was the major contributor to the computational cost.

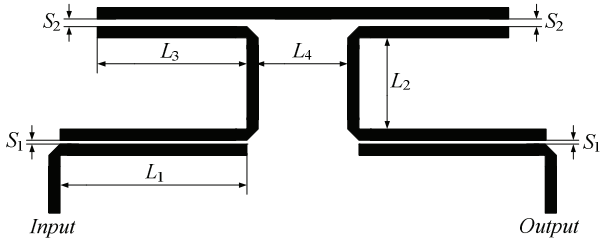

Fig. 12. Coupled-line bandpass filter: geometry [23].

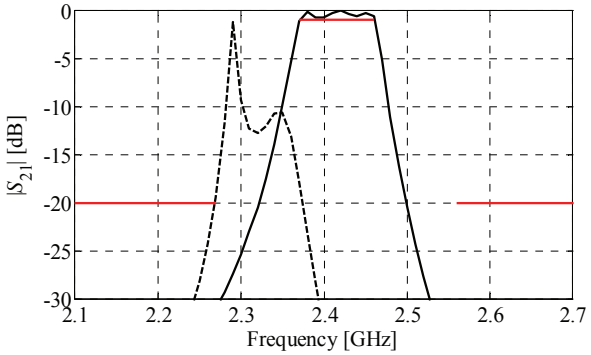

Fig. 13. Coupled-line bandpass filter: responses of $\boldsymbol{R}_{c.1}$ at the initial design $\boldsymbol{x}^{(0)}$ (dashed line) and at its optimized design $\boldsymbol{x}^{(1)}$ (solid line), as well as the response of $\boldsymbol{R}_{c.2}$ at $\boldsymbol{x}^{(0)}$ (dotted line); design specifications are adjusted to absorb the frequency shift between $\boldsymbol{R}_{c.1}(\boldsymbol{x}^{(0)})$ and $\boldsymbol{R}_{c.2}(\boldsymbol{x}^{(0)})$.

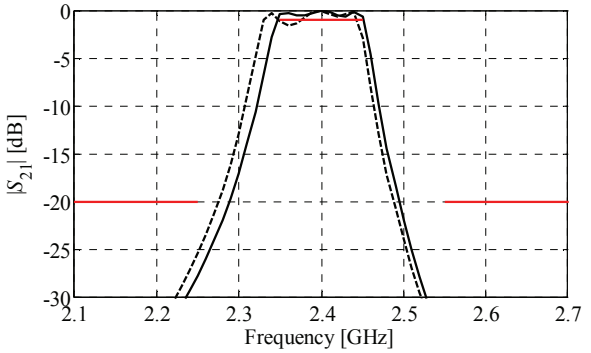

Fig. 14. Coupled-line bandpass filter: responses of the coarse-discretization model $\boldsymbol{R}_{c.2}$ at $\boldsymbol{x}^{(1)}$ (dashed line) and at its optimized design $\boldsymbol{x}^{(2)}$ (solid line), as well as the response of $\boldsymbol{R}_f$ at $\boldsymbol{x}^{(2)}$ (dotted line).

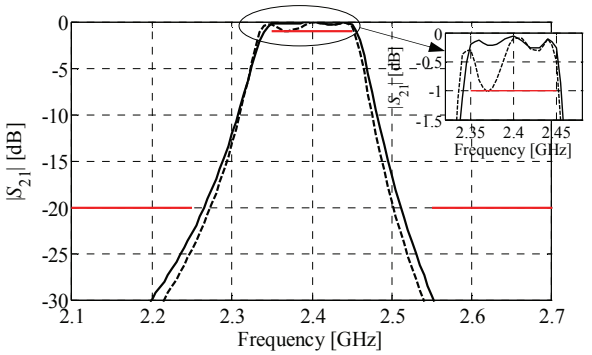

Fig. 15. Coupled-line bandpass filter: responses of the fine-discretization model $\boldsymbol{R}_f$ at $\boldsymbol{x}^{(2)}$ (dashed line) and at the refined final design $\boldsymbol{x}^*$ (solid line); here the original design specifications are shown.

D. Comparison with Direct Optimization

In order to illustrate the computational efficiency of the proposed technique, the fine models for the three filter examples have been directly optimized using the pattern-search algorithm of Section II.A. The results are presented in Table 4. In all cases, the design found by direct search is similar to that obtained using our method (specification errors –2.1 dB, –0.025, and –1.8 dB, respectively). However, the computational cost, depending on the example, is 10 to 20 times higher than that for the technique presented here.

Table 4: Direct fine model optimization results.

Example	CPU Cost	
	$\boldsymbol{R}_f$ Calls	Time
Stacked slotted resonators filter (III.*A*)	120	32 h
HTS filter (III.*B*)	210	179 h
Coupled-line bandpass filter (III.*C*)	133	95 h

IV. CONCLUSION

A simple and robust algorithm for microwave design optimization is proposed that exploits sequential, multi-grid optimization of coarse-discretization EM-simulation-based models and polynomial-approximation-based refinement of the final design. The presented method is easy to implement. It does not need any auxiliary equivalent-circuit model (which is typically used by space mapping) or any modifications of the original structure, such as cutting and inserting the tuning ports necessary by the tuning methodology. It is also computationally efficient, as most of the operations are performed on the coarse-discretization models. Because of its simplicity and versatility, the proposed method can be viewed as a step forward towards making simulation-driven microwave design feasible and computationally tractable.

ACKNOWLEDGMENT

The author thanks Sonnet Software, Inc., Syracuse, NY, for making ***em***™ available. This work was supported in part by the Reykjavik University Development Fund under Grant T09009.

REFERENCES

[1] R.V. Snyder, "Practical aspects of microwave filter development," *IEEE Microwave Magazine*, vol. 8, no. 2, pp. 42-54, Apr. 2007.

[2] A. Bhargava, "Designing circuits using an EM/circuit co-simulation technique," *RF Design*, p. 76, Jan. 2005.

[3] S. Shin and S. Kanamaluru, "Diplexer design using EM and circuit simulation techniques," *IEEE Microwave Magazine*, vol.8, no.2, pp.77-82, Apr. 2007.

[4] N. V. Queipo, R. T. Haftka, W. Shyy, T. Goel, R. Vaidynathan, and P.K. Tucker, "Surrogate-based analysis and optimization," *Progress in Aerospace Sciences*, vol. 41, no. 1, pp. 1-28, Jan. 2005.

[5] A. I. J. Forrester and A. J. Keane, "Recent advances in surrogate-based optimization," *Prog. in Aerospace Sciences*, vol. 45, no. 1-3, pp. 50-79, Jan.-April, 2009.

[6] J. W. Bandler, Q. S. Cheng, S. A. Dakroury, A. S. Mohamed, M. H. Bakr, K. Madsen, and J. Søndergaard, "Space mapping: the state of the art," *IEEE Trans. Microwave Theory Tech.*, vol. 52, no. 1, pp. 337-361, Jan. 2004.

[7] S. Amari, C. LeDrew, and W. Menzel, "Space-mapping optimization of planar coupled-resonator microwave filters," *IEEE Trans. Microwave Theory Tech.*, vol. 54, no. 5, pp. 2153-2159, May 2006.

[8] G. Crevecoeur, L. Dupre, and R. Van de Walle, "Space mapping optimization of the magnetic circuit of electrical machines including local material degradation," *IEEE Trans. Magn.*, vol. 43, no 6, pp. 2609-2611, June 2007.

[9] D. Echeverria and P. W. Hemker, "Space mapping and defect correction," *CMAM The International Mathematical Journal Computational Methods in Applied Mathematics,* vol. 5, no. 2, pp. 107-136, 2005.

[10] S. Koziel, J. W. Bandler, and K. Madsen, "A space mapping framework for engineering optimization: theory and implementation," *IEEE Trans. Microwave Theory Tech.*, vol. 54, no. 10, pp. 3721-3730, Oct. 2006.

[11] S. Koziel, Q. S. Cheng, and J. W. Bandler, "Space mapping," *IEEE Microwave Magazine*, vol. 9, no. 6, pp. 105-122, Dec. 2008.

[12] X. J. Zhang and D. G. Fang, "Using circuit model from layout-level synthesis as coarse model in space mapping and its application in modelling low-temperature ceramic cofired radio frequency circuits," *Microwaves, Antennas & Propagation, IET*, vol. 1, no. 4, pp. 881-886, Aug. 2007.

[13] D. Swanson and G. Macchiarella, "Microwave filter design by synthesis and optimization," *IEEE Microwave Magazine*, vol. 8, no. 2, pp. 55-69, Apr. 2007.

[14] J. C. Rautio, "EM-component-based design of planar circuits," *IEEE Microwave Magazine*, vol. 8, no. 4, pp. 79-90, Aug. 2007.

[15] J. C. Rautio, "Perfectly calibrated internal ports in EM analysis of planar circuits," *IEEE MTT-S Int. Microwave Symp. Dig.*, pp. 1373-1376, June 2008.

[16] S. Koziel, J. Meng, J. W. Bandler, M.H. Bakr, and Q.S. Cheng, "Accelerated microwave design optimization with tuning space mapping," *IEEE Trans. Microwave Theory and Tech.*, vol. 57, no. 2, pp. 383-394, 2009.

[17] Q. S. Cheng, J. W. Bandler, and S. Koziel, "Tuning Space Mapping Optimization Exploiting Embedded Surrogate Elements," *IEEE MTT-S Int. Microwave Symp. Dig*, pp. 1257-1260, 2009.

[18] S. Koziel, J. W. Bandler, and K. Madsen, "Quality assessment of coarse models and surrogates for space mapping optimization," *Optimization and Engineering*, vol. 9, no. 4, pp. 375-391, 2008.

[19] ***em***™ Version 12.54, Sonnet Software, Inc., 2009.

[20] N. M. Alexandrov and R. M. Lewis, "An overview of first-order model management for engineering optimization," *Optimization Eng.*, vol. 2, no. 4, pp. 413-430, Dec. 2001.

[21] C. L. Huang, Y. B. Chen, and C. F. Tasi, "New compact microstrip stacked slotted resonators bandpass filter with transmission zeros using high-permittivity ceramics substrate," *Microwave Opt. Tech. Lett.*, vol. 50, no. 5, pp. 1377-1379, May 2008.

[22] J. W. Bandler, R. M. Biernacki, S. H. Chen, R. H. Hemmers, and K. Madsen, "Electromagnetic optimization exploiting aggressive space mapping," *IEEE Trans. Microwave Theory Tech.*, vol. 43, no.12, pp. 2874-2882, Dec. 1995.

[23] H. M. Lee and C. M. Tsai, "Improved coupled-microstrip filter design using effective even-mode and odd-model characteristic impedances," *IEEE Trans. Microwave Theory Tech.*, vol. 53, no. 9, pp. 2812-2818, Sept. 2005.

[24] FEKO® *User's Manual*, Suite 5.3, EM Software & Systems-S.A. (Pty) Ltd, http://www.feko.info, 2008.

Slawomir Koziel received the M.Sc. and Ph.D. degrees in electronic engineering from Gdansk University of Technology, Poland, in 1995 and 2000, respectively. He also received the M.Sc. degrees in theoretical physics and in mathematics, in 2000 and 2002, respectively, as well as the PhD in mathematics from the University of Gdansk, Poland in 2003. He is currently an Associate Professor with the School of Science and Engineering, Reykjavik University, Iceland. His research interests include CAD and modeling of microwave circuits, surrogate-based optimization, space mapping, circuit theory, analog signal processing, evolutionary computation and numerical analysis.